frontiers | Frontiers in Environmental Science

TYPE Original Research
PUBLISHED 09 May 2025
DOI 10.3389/fenvs.2025.1555628

Check for updates

OPEN ACCESS

EDITED BY
Xiao Liu,
South China University of Technology, China

REVIEWED BY
Grazia Masciandaro,
National Research Council (CNR), Italy
Li Li,
Guangzhou University, China

*CORRESPONDENCE
Yongjun Shi,
✉ 19940009@zafu.edu.cn

RECEIVED 11 January 2025
ACCEPTED 09 April 2025
PUBLISHED 09 May 2025

CITATION
Zhang R, Cheng X, Chen W, Lu F, Liu S, Shi H, Ni Z, Chen Y, Li D, Zhou Y and Shi Y (2025) Effects of different urban vegetation cover and green space types on soil greenhouse gas emissions and carbon sequestration. *Front. Environ. Sci.* 13:1555628. doi: 10.3389/fenvs.2025.1555628

Effects of different urban vegetation cover and green space types on soil greenhouse gas emissions and carbon sequestration

Ruisha Zhang[1,2,3], Xuekun Cheng[1,2,3], Wu Chen[4], Feng Lu[5], Shuhan Liu[1,2,3], Haitao Shi[1,2,3], Zelong Ni[1,2,3], Yangen Chen[6], Dabiao Li[7], Yufeng Zhou[1,2,3,8] and Yongjun Shi[1,2,3,8]*

[1]State Key Laboratory of Subtropical Silviculture, Zhejiang A&F University, Hangzhou, China, [2]Key Laboratory of Carbon Cycling in Forest Ecosystems and Carbon Sequestration of Zhejiang Province, Zhejiang A&F University, Hangzhou, China, [3]School of Environmental and Resources Science, Zhejiang A&F University, Hangzhou, China, [4]Baiyunshan Forest Farm, Lishui, China, [5]Yuhang District Forestry and Water Conservancy Bureau of Hangzhou, Hangzhou, China, [6]Agriculture and Rural Bureau of Lin'an District, Hangzhou, China, [7]Suichang County Natural Resources and Planning Bureau, Suichang, China, [8]Zhejiang Province Key Think Tank, Institute of Ecological Civilization, Zhejiang A&F University, Hangzhou, China

The development of urbanization has led to the creation of various types of green spaces, which have a direct influence on vegetation types and soil management, This, in turn, results in differences in soil carbon sequestration capacities. However, the factors affecting soil carbon sequestration in different vegetation types within urban green spaces remain largely unexplored. To address this gap, the study focused on the soil of urban green space. A one-year field observation was conducted, utilizing local management archives and historical data, to evaluate variations in soil greenhouse gas (GHG) emission and soil organic carbon sequestration across grassland (GL), shrubs (SH), and forests stands (FS) within three types of green spaces: park green space (P), residential green space (Ra), and street green space (s). The results indicated that: (1) In comparison to grassland (GL), the CO_2 flux of shrubs (SH) and forests stands (FS) declined by 10.73% and 14.46%, respectively, while the N_2O and CH_4 fluxes remained insignificant. Additionally, the annual increase in soil organic carbon was lower by 8.92% and 10.80% in shrub and forests stand, respectively; (2) Variations in greenhouse gas fluxes were also observed among the three types of green spaces. In comparison to park green spaces, the CO_2 flux of residential and street soils decreased by 2.11% and 3.25%, respectively, while the N_2O flux dropped by 16.61% and 22.41%, respectively. The CH_4 flux remained insignificant. The annual increase of SOC in residential and streets was notably lower than that in parks green spaces, by 9.59% and 15.20%, respectively, indicating significant differences. This suggests that soil carbon sequestration capacity is highly responsive to changes in vegetation coverage and green space types, with WSOC, NH_4^+-N, and pH identified as the primary factors influencing the greenhouse gas flux in the three soils. This study provides data and a theoretical basis for the strategic selection of urban soil management measures, particularly in the context of achieving carbon neutrality goals.

KEYWORDS

urban green space (UGS), vegetation cover, soil carbon sequestration, soil GHG fluxes, urban soil

1 Introduction

Although cities account for only about 2% of the world's land area, they contribute roughly 70% of global carbon emissions (Churkina, 2016). The negative impacts of urbanization have exacerbated the tension between the environment and humans (Yang et al., 2023). To mitigate the negative impacts of these emissions, increasing carbon storage in urban areas is essential (Churkina et al., 2010). Urban green spaces, as key public open areas, not only provide a place for the public for recreation, relaxation, and enjoyment, but also play a crucial role in enhancing the quality of life for city residents. Furthermore, they hold significant ecological importance in maintaining biodiversity, fixing greenhouse gases in the atmosphere, and mitigating the urban heat island effect (Aram et al., 2019; Aronson et al., 2017; Zhang and Qian, 2024) Therefore, green infrastructure has been recognized as an effective strategy to address urban environmental issues (Lal and Augustin, 2012). Soil not only supports the physical development of green infrastructure but also collaborates with vegetation to facilitate the carbon and nitrogen cycles within urban ecosystems, thus playing a key role in determining the environmental quality of green infrastructure (Morel et al., 2015). However, in the process of expanding green infrastructure, urban functional block construction often introduces various vegetation combinations and management models, which can lead to significant alterations in the soil activities of these green spaces (Liu et al., 2023; Reynolds et al., 2020; Schetke et al., 2016). Research indicates that tree species diversity in forest will significantly increase the soil carbon sequestration (Zhang X. et al., 2024), while soil degradation resulting from the unmanagement can substantially reduce the gas flux of the soil (Yuan et al., 2023).

Soil carbon sequestration is crucial for mitigating global climate change and maintaining the ecosystem balance (Liu Q. et al., 2024). Soil organic carbon, a primary source of soil nutrients, is mainly decomposed by microorganisms and subsequently stored in the soil, helping to fix atmospheric CO_2. Thus, SOC has become an ideal indicator for assessing soil carbon sequestration (Zhu et al., 2020). Numerous studies have highlighted diverse factors driving the accumulation of urban soil organic carbon (Vasenev and Kuzyakov, 2018). For instance, (Chen X. et al., 2022). analyzed surface litter and soil samples from six urban and suburban forests in China, classifying soil organic carbon and quantitatively assessing the content of each organic carbon group. Their study revealed that urbanization significantly influences the accumulation pattern of

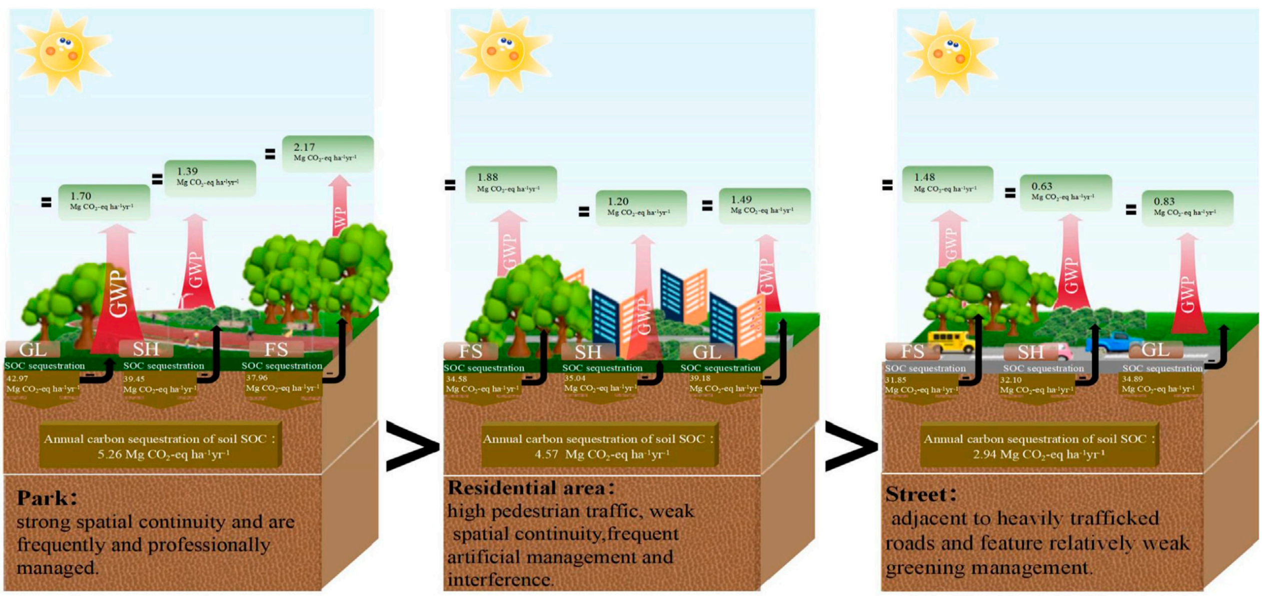

GRAPHICAL ABSTRACT
The research focuses on urban green space soil, investigating the variations in soil carbon sequestration capacity across different green space types and vegetation coverages. The findings revealed significant variations in soil carbon sequestration functionality among various green space types and vegetation coverages. The maximum soil carbon sequestration was observed in the park type with forest planting. Consequently, to enhance soil carbon sequestration, it is necessary to augment the coverage area of diverse vegetation and management intensity of greenspace in the process of urban construction to enhance the carbon sink function of the soil, in order to maintain the balance of the urban ecosystem.

SOC in subtropical forest surface soils, such as shifting from microbial-mediated pathways to abiotic pathways, which impact the stability of soil organic carbon. Similarly, (Chaurasia et al., 2023) compared the effects of five urban land use patterns on soil SOC accumulation, found that soil SOC accumulation varies significantly among the five land use categories.

There is a high correlation between soil carbon sequestration capacity and soil GHG flux (Rubaiyat et al., 2023; Serrano-Silva et al., 2014). However, most existing studies on the response of soil carbon sequestration to urban environmental changes primarily focus on soil organic carbon content, The dynamic changes in soil characteristics across different urban vegetation coverage types. Remain largely unexplored (Enescu et al., 2022). Therefore, it is necessary to conduct dynamic research on soil physical and chemical properties, as well as GHG fluxes, in urban green space types influenced by different vegetation coverage types (Serrano-Silva et al., 2014). This approach not only emphasizes the shaping of soil environment by changes in vegetation coverage types, but also is related to the specific activity state of soil. Integrating the dynamic changes in soil carbon and nitrogen pools with soil GHG emissions will provide a comprehensive understanding of the changes and mechanisms affecting soil activity in urban green space during urbanization. This will also aid in formulating more effective management strategies for different urban green space types (Demuzere et al., 2014).

Many uncertainties remain regarding the mechanism through which vegetation coverage and green space usage influence soil carbon sequestration function. The functional classification of green space, as well as the interactions between aboveground vegetation and the soil carbon and nitrogen pools, requires further investigation (Liu Y. et al., 2024). In light of this, the present study conducted a one-year-long field observation to examine the differences in soil GHG flux and soil carbon pool across three vegetation coverage types: grassland (GL), shrub (SH) and forest stands (FS). These types were studied in three green space categories: park green space (P), residential area green space (Ra), and street green space (S). This research aims to explore how environmental factors in the soil vary across different vegetation coverage and green space types, and how these factors influence GHG flux mechanism. The goal is to provide a reliable reference for optimizing urban green space management, rational urban green space planning, and the construction of low-carbon cities.

2 Materials and methods

2.1 Experiment region

The experimental site was situated in Lin'an District, Hangzhou City, Zhejiang Province (119°50′E longitude and 30°14′N latitude) (Figure 1). The region has a subtropical monsoon climate, characterized by four distinct seasons. Summers are hot and receive abundant rainfall, while winters are relatively cool. The mean annual temperature (MAT) is 15.6°C, 15.6°C, and the mean annual precipitation (MAP) measured 1,450 mm. The frost-free period lasted for approximately 230 days, with a total sunshine duration of 1847 h. According to Chinese classification standards, the soil in this area is classified as krasnozem (Lv et al., 2022).

2.2 Experiment design

In accordance with China's "Urban Green Space Classification Standard" (CJJ/T85–2017) as cited in (Cjj/t 85–2017, 2018). Among these, the "park green space" pertains to the G132 category within the urban green space classification standard, featuring a highly integrated distribution pattern and a green space coverage rate of ≥80%; The "residential area green space" falls under the RG category in the urban green space classification standard, exhibiting diverse distribution forms and a greening coverage area of ≥65%; The "street green space" belongs to the SG category in the urban green space classification standard, with a greening coverage area of ≥40%. Subsequently, based on field surveys, sample plots under three types of vegetation cover: shrubs, grassland, and forest stand were further selected. In March 2023, plots were established at selected locations, each having an area of 100 m^2. The minimum distance between each plot was set at 200 m (Figure 1). In forest stand (FS), the dominant tree species within the forest are all indigenous dominant tree species in Zhejiang Province, and the soil has an establishment history of approximately 10 years. In order to more effectively reflect the activity patterns of greenhouse gas fluxes and environmental factors, we carried out continuous field observations for 12 months (from April 2023 to March 2024) within the sample plot.

A fundamental survey of the vegetation within the plot was carried out. The principal constituents of the survey encompassed vegetation, diameter at breast height, coverage, and biomass. The diameter at breast height is defined as the diameter of the tree trunk measured at breast height above the ground surface (Zhang et al., 2023). The ground diameter is denoted as the diameter of the tree trunk base just above the ground, commencing from the ground level. The ground diameters of standing trees and shrubs were measured employing traditional surveying methodologies. A DBH ruler was utilized to measure 130 cm above the base of the tree trunk, while the ground diameter of shrubs was measured at 10 cm above the ground. With respect to the average height, the direct measurement approach was adopted for shrubs and grass. Locate a flat area on the ground, hold the ruler perpendicularly to the ground surface such that the scale line aligns with the apex of vegetation growth, and subsequently read the measurement indicated on the ruler. The average height of the forest patch was gauged employing an altimeter. Measuring points were randomly chosen within each plot, and the measurement process was repeated thrice (Supplementary Table S1).

The coverage degree primarily refers to the percentage of the vertical projected area of the above-ground portion of the plant in relation to the sample plot area, as reported in (Peaden, 2019). Vegetation coverage was quantified using the coverage box method. On sunny days, between 12:00 and 15:00 p.m., a 1 m × 1 m quadrat frame was randomly positioned within the quadrat area, and the area covered by the vertical projection of vegetation within the frame was observed and recorded. The vegetation coverage was calculated by comparing the coverage area with the total frame area. Given that the projection of the grassland is nearly imperceptible, the green coverage area within the quadrat frame was used as a substitute. This procedure was repeated three times for each quadrat (Supplementary Table S1).

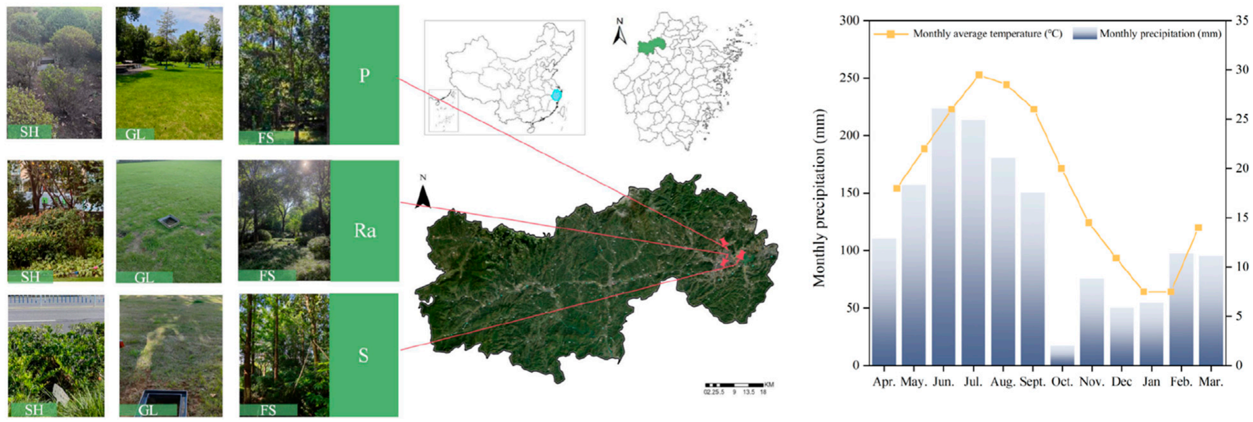

FIGURE 1
It shows the location of the sample plots in this study. SH, GL and FS represent shrub, grassland and forest stand, and P, Ra, S represent Park green space, Residential area green space and Street green space, respectively. The right figure shows in the mean monthly temperature and mean monthly precipitation throughout the experiment month.

Biomass is defined as the total dry weight of organic matter that persists per unit area or volume at a specific time, as noted in (Ónodi et al., 2017). Different biomass measurement methods are used based on vegetation cover types. The biomass of grassland and shrubs was measured using the harvest sampling method. A small 25 cm × 25 cm quadrat was placed within the sample plot. Sampling tools were used to collect soil from the surface layer, extending from the above-ground vegetation to a depth of 0–20 cm below ground level in the quadrat,The specimens were then transported to the laboratory, where plant components were separated from the soil, weighed, and placed in an oven at 105°C for 12 h. After drying, the biomass value was converted into area and weight units to determine the biomass per unit area (kg C m^{-2}). This process was repeated three times. The forest standing biomass in the arboreal zone is calculated using a model-based protocol. Based on the diameter at breast height and tree species data from the sample plot, the volume was estimated using the volume table specific to Zhejiang Province. The BEF conversion coefficient (for fir, Masson pine, hard broadleaf, soft broadleaf) was calculated using 2009 CFI data (values of 0.7453, 0.8839, and 1.0705 respectively). The total biomass in the forest stand was then obtained, and the area and weight units were converted to determine the standing tree biomass per unit area of the sample plot (kg C m^{-2}) (Supplementary Table S1).

2.3 Soil sampling and determination of environmental factors

Soil sampling was conducted during the even-numbered months of the observation period, to ensure the data's representativeness, a random sampling method was applied. Firstly, the central point of each sample plot was designated as the sampling center. Then, four equally spaced points were selected along the diagonal from this center. Soil samples were collected from the 0–10 cm layer at each of these five points. After collection, the soil from all five points was thoroughly mixed to ensure uniformity. This sampling procedure was repeated three times at each point. In total,162 soil samples were collected over the observation period.

Once the collected samples were transported to the laboratory, they underwent a series of processing steps. The samples were divided into four portions. One portion was immediately stored at −40°C for cryopreservation. A second portion was sieved through a 2-mm sieve and then stored in a 4°C refrigerator. To ensure sample stability for subsequent analysis of soil carbon and nitrogen. From the remaining sample, 10–15 g of fresh soil was weighed, prepared for pH measurement. For the pH determination, the potentiometric method was used. Ten grams of air-dried soil, sieved through a 2-mm sieve and air-dried for 2 weeks, were mixed with 25 mL of ultrapure water, the mixture was stirred for 1–2 min, allowed to stand for 30 min, and then the pH was measured using a calibrated pH meter (FE20; Mettler Toledo, Switzerland) (Aramburu Merlos et al., 2023).

Soil microbial carbon (MBC; mg kg^{-1}) and microbial nitrogen (MBN; mg kg^{-1}) were determined using the chloroform fumigation extraction method (TOC-VcpH; Shimadzu; Kyoto, Japan) (Liao et al., 2021). Water-soluble carbon (WSOC) and water-soluble nitrogen (WSON) were measured employing the Singh (Wang et al., 2022) method with a TOC-TN automatic analyzer (TOC-VcpH, Shimadzu, Kyoto, Japan). Ammonium nitrogen (NH_4^+-N) (mg kg^{-1}) and nitrate nitrogen (NO_3^--N) (mg kg^{-1}) concentrations were determined using the indophenol blue colorimetric method and dual-wavelength ultraviolet spectrophotometry, respectively, with a spectrophotometer (UV-8000 P C, Shanghai, China) (Rouge, 1981).

In April 2023 and March 2024, three portions of soil from the surface stratum 0–20 cm were randomly sampled from each sampling point to measure soil organic carbon storage. We used the following Formula 1 to calculate soil organic carbon stocks (Wang et al., 2004):

$$C_{SOC} = \sum_i^n C_i \times B_i \times D_i \times 100^{-1} \tag{1}$$

In the formula, C_{SOC} represents the SOC reserve (Mg C ha^{-1}) in the 0–20 cm soil, i represents the specific soil stratum. C_i represents the organic carbon concentration (g kg^{-1}) at depth i, B_i represents the soil bulk density (g cm^{-3}) at depth i, and D_i represents the soil thickness (cm) at depth i. Soil thickness and soil bulk density (g cm^{-3}) are also considered in the formula.

The annual carbon sequestration of soil organic carbon was calculated using Equation 2:

$$\Delta_{SOC} = \frac{44}{12} \times (C_{SOC,2024} - C_{SOC,2023}) \quad (2)$$

Where Δ_{SOC} depicts the annual soil carbon sequestration (CO_2-eq Mg ha^{-1} $year^{-1}$); $C_{SOC,2024}$ and $C_{SOC,2023}$ depict soil organic carbon storage in 2024 and 2023, respectively.

2.4 Measurements of soil GHG emissions

Greenhouse gas flux in the study area was measuring using the closed static chamber-gas chromatography method. During the observation period, an experimental device constructed from PVC was installed in the study area. This device consisted of a base and a chamber. With the chamber measured 30 cm × 30 cm ×30 cm and featuring a 1 cm diameter hole at the center of its top, a rubber stopper was inserted into this hole for gas sampling. The base, measuring 30 cm × 30 cm×10 cm, included a 5 cm × 5 cm groove on its top and was embedded 0–10 cm into the soil. Prior to installation, plant stems, leaves, and roots within the embedding area were thoroughly eliminated to remove the effects of plant respiration.

Sampling was conducted from 8:00 to 11:00 a.m. on sunny days each month. Before sampling, vegetation within the base area was trimmed with scissors, and a fan was placed inside the base area. Then, approximately 800 mL of ultrapure water was poured into the groove. The chamber, with the hole facing upward, was then placed into the groove, and gas sampling was initiated using a medical syringe. Gas samples were collected every 10 min at 0, 10, 20, and 30 min. With each sample totaling 80 mL which was stored in a 100 mL sealed aluminum foil bag. Simultaneously, along with the greenhouse gas sampling, a soil thermometer (Dalian Bright Chemical Design Institute, Dalian, China) was vertically inserted into the soil to a depth of 5 cm, and close to the box, to measure the soil temperature. Each sample was tested in triplicate to calculate the standard deviation of the experimental data. After collecting the experimental samples, the gas samples were promptly analyzed within 48 h using a Shimadzu Gas Chromatograph (GC-2014, Shimadzu Corporation, Tokyo). The concentrations of greenhouse gases in the samples were quantified by measuring them against a standard curve established using laboratory reference standards. The standard concentrations used were as follows: N_2O:5.0 × 10^{-6} mol/mol, CH_4:20.4 × 1010^{-6} mol/mol, CO_2:302 × 1010^{-6} mol/mol The following Formula 3 is used to calculate the concentrations of N_2O, CH_4, CO_2 (Song et al., 2020):

$$F = \rho \times \frac{V}{A} \times \frac{P}{P_0} \times \frac{dC_t}{d_t} \times \frac{T_0}{T} \quad (3)$$

Where F represents the soil greenhouse gas emission flux ($mg \cdot m^{-2} \cdot h^{-1}$), ρ represents the greenhouse gas concentration value under standard laboratory reference conditions. A (m^2) V (m^3) are the effective bottom area and volume of the chamber, respectively; $\frac{P}{P_0}$ is the ratio of atmospheric pressure under standard conditions to atmospheric pressure in the laboratory. $\frac{T_0}{T}$ It is the ratio of the absolute temperature under standard conditions to the absolute temperature inside the PVC box during sampling.

The annual greenhouse gas emissions are calculated by the following formula (Xu et al., 2020):

$$F_g = \frac{\sum (F_{i+1} + F_i)}{2} \times (t_{i+1} - t_i) \times 24 \times 10^{-5} \quad (4)$$

In the formula, F_g represents the soil CO_2, N_2O emissions, or CH_4 uptake (Mg CO_2 ha^{-1} yr^{-1}, kg N_2O and CH_4 ha^{-1} yr^{-1}); F represents the emission of each soil GHG determined at each sampling time, i represent the sample number, and t represents the sampling time.

The global warming potential (GWP) was used to assess the contribution of soil greenhouse gas fluxes to global warming under the three types of coverage. The calculation method is as follows Formula 5 (Xu et al., 2020):

$$GWP_T = F_{CO_2} + F_{CH_4} \times 25 + F_{N_2O} \times 298 \quad (5)$$

In the formula, F_{CO_2}, F_{CH_4}, F_{N_2O} respectively represent the cumulative emissions of CO_2, CH_4, and N_2O. The numbers 25 and 98 are the conversion factors for the emission fluxes of CH_4 and N_2O to be equivalent to the emission of CO_2 over a 100-year time scale.

2.5 Determination of the soil carbon sequestration

Soil carbon sequestration refers to the ability of soil to absorb and store carbon dioxide. In this study, soil carbon sequestration is defined as the total amount of carbon stored in the soil carbon pool, after accounting for the carbon dioxide emitted from soil greenhouse gases during the experimental period. The annual soil carbon sequestration in this study was calculated using the following Equation 6:

$$U_{total} = \Delta_{SOC} - GWP \quad (6)$$

Where U_{total} refers to the yearly carbon sequestration of the soil in different urban vegetation cover and green space types, Δ_{SOC} and GWP represent soil SOC sequestration, and the soil GHG emissions.

2.6 Statistical analyses

Preliminary data recording and classification were performed using Excel. The data were analyzed using SPSS 26.0, and the significance level was set at 0.05. Prior to data analysis data analysis, One-way analysis of variance (ANOVA) and least significant difference (LSD) were employed to compare the differences in soil carbon and nitrogen pools as well as soil carbon sequestration under different vegetation coverage and green space types. The responses of soil greenhouse gas emissions, soil temperature, soil water content, water-soluble organic carbon (WSOC), NO_3^--N, NH_4^+-N, microbial biomass

TABLE 1 The differences (mean ± standard deviation, n = 3) in soil environmental factors under different vegetation cover types were analyzed. Additionally, the responses of soil environmental factors and annual greenhouse gas emissions to seasonal changes were assessed under various urban vegetation cover and green space types using repeated measures analysis of variance (RM-ANOVA).

UGS	Treatment	M (g kg^{-1})	pH	T (°C)	WSOC (mg kg^{-1})	MBC (mg kg^{-1})	WSON (mg kg^{-1})	MBN (mg kg^{-1})	NH_4^+-N (mg kg^{-1})	No$_3^-$-N (mg kg^{-1})	CH_4 uptake (μg m^{-2} h^{-1})	N_2O emission (μg m^{-2} h^{-1})	CO_2 emission (mg m^{-2} h^{-1})
Park	SH	22.75 ± 0.33b	6.77 ± 0.41b	7.8 ± 0.03c	168 ± 1.27b	199.24 ± 6.72b	17.42 ± 0.19c	22.73 ± 0.03b	11.25 ± 0.08b	9.13 ± 0.48b	43.661 ± 2.05b	69.68 ± 3.85b	412.51 ± 14.21b
	GL	22.83 ± 0.25b	6.98 ± 0.60a	9.52 ± 0.05a	170.17 ± 2.99b	230.27 ± 0.71a	20.1 ± 0.19a	30.05 ± 6.07a	12.28 ± 0.18a	12.06 ± 0.26a	45.51 ± 1.23a	75.96 ± 2.62a	447.14 ± 12.69a
	FS	24.14 ± 0.27a	6.81 ± 0.77b	8.51 ± 0.33b	172.82 ± 1.18a	200.59 ± 1.28b	19.74 ± 0.10b	22.05 ± 6.85b	11.18 ± 0.11b	9.54 ± 0.25b	40.62 ± 01.22b	68.36 ± 3.93b	387.05 ± 4.01c
Residential area	SH	22.08 ± 0.31a	5.77 ± 0.02b	9.07 ± 0.02c	156.29 ± 3.18a	202.5 ± 5.43a	15.25 ± 0.15b	24.3 ± 0.03c	8.87 ± 0.15b	5.69 ± 0.07c	43.02 ± 1.62a	59.53 ± 2.97ab	367.69 ± 8.16b
	GL	20.56 ± 1.69a	5.86 ± 0.02a	10.29 ± 0.03a	159.1 ± 4.86a	203.01 ± 4.17a	16.95 ± 0.29a	27.2 ± 0.08b	9.59 ± 0.002a	9.28 ± 0.04a	43.69 ± 0.82a	66.31 ± 3.69a	409.34 ± 5.64a
	FS	21.48 ± 0.35a	5.64 ± 0.02c	9.5 ± 0.09b	159.21 ± 3.71a	184.06 ± 2.98b	16.36 ± 0.67a	28.3 ± 0.08a	8.72 ± 0.03b	9.08 ± 0.85b	39.71 ± 0.74b	52.6 ± 4.31b	356.69 ± 7.85b
Street	SH	23.36 ± 0.20b	5.79 ± 0.01b	11.11 ± 0.10b	142.81 ± 1.41a	167.31 ± 1.11a	14.65 ± 0.17a	24.78 ± 0.03a	7.18 ± 0.40c	5.21 ± 0.10c	41.57 ± 0.94a	56.8 ± 2.52a	341.46 ± 21.42b
	GL	25.8 ± 0.35a	5.96 ± 0.03a	12.26 ± 0.008a	143.54 ± 0.47a	170.14 ± 1.92a	14.86 ± 0.13a	22.47 ± 0.06b	9.2 ± 0.07a	7.85 ± 0.04a	42.89 ± 1.03a	59.46 ± 5.25a	370.1 ± 4.03a
	FS	21.72 ± 1.42b	5.79 ± 0.01b	11.08 ± 0.04b	143.99 ± 2.07a	170.21 ± 9.01a	14.68 ± 0.28a	23.69 ± 0.03c	8.47 ± 0.08b	6.65 ± 0.12b	41.55 ± 1.36a	49.77 ± 1.76b	331.05 ± 2.70b
Analysis of seasonal changes		ns	ns	***	***	***	***	***	***	***	ns	***	***

Notes: T represents the soil temperature at a depth of 5 cm; M represents soil moisture content, and MBC, MBN, and WSOC, respectively stand for the concentrations of microbial C and N as well as water-soluble organic C. Different letters within a column indicate significant differences among different vegetation cover types under different green space types, based on the least significant difference (LSD) test, P = 0.05. Ns, ***, and respectively indicate significant differences when P < 0.001.

10.3389/fenvs.2025.1555628

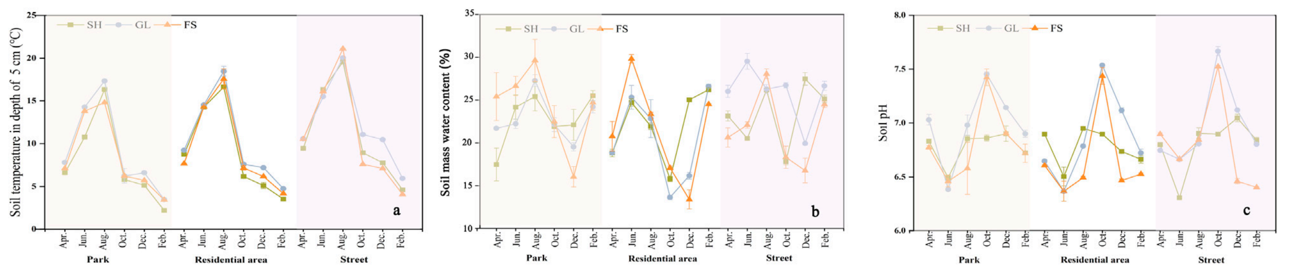

FIGURE 2
Monthly changes of soil environmental factors under different types of greenspace covered by vegetation. Soil temperature (**a**), soil moisture content (**b**), and soil pH (**c**). These values represent means ± SDs (n = 3).

carbon (MBC), and microbial biomass nitrogen (MBN) to seasonal changes were analyzed using repeated measures analysis of variance (RM-ANOVA) and tests. PCA (Principal Component Analysis; PCA) was applied to analyze the correlation between soil physical and chemical properties and C and N pool; To assess the interactive effects of different vegetation cover and green space types on soil carbon and nitrogen pools, as well as greenhouse gas emissions, HLM (Hierarchical Linear Model; HLM) was used, with green space type treated as a random effect. Lastly, redundancy analysis (RDA) and Random Forest were used to investigate the relationship between soil greenhouse gas fluxes under different green space types. The presentation of soil physical and chemical properties and statistical charts in this article was completed by Origin 2018.

3 Results

3.1 Effects of different types of urban vegetation covering green space on soil physical and chemical properties and C and N pools

Over a 12-month period of field observations, the fluctuation pattern of soil temperature at a depth of 5 cm showed a strong correlation with the seasonal temperature change in the study area. The lowest temperature occurred in winter (December-February), while the highest temperature was observed in summer (August) (Table 1; Figure 2a). Significant differences in soil temperature and pH were found among various vegetation covers, with lower soil pH and temperature observed under forest stand (FS) (Figure 2). Notably, in park types (P), the differences in soil temperature and pH among vegetation cover types were more pronounced ($p < 0.05$) Additionally, the HLM results indicate that the interaction between green space type and vegetation cover has a significant effect on soil pH and temperature ($p < 0.05$) (Table 2). Significant differences in soil moisture content were observed among different vegetation cover types only in the residential area (Ra), while the differences in soil moisture content between vegetation covers were not significant in the other green space types (Table 1). Overall, compared with park type, the soil pH of residential area (Ra) and street (S) types decreased by 15.0% and 13.89%, respectively (Table 2). Notably, the soil pH under grassland (GL) coverage exhibited a statistically significant increase ($p < 0.05$).

Soil C pool movement responded similarly to seasonal changes (Table 1; Figure 3). Differences in mean monthly WSOC content between vegetation covers within the same green space type varied minimally. However, in the park type(P), the mean monthly WSOC content of the forest stand (FS) was 172.82 ± 1.18 mg kg^{-1}, which was significantly ($p < 0.05$) higher by 1.5% and 3.1% compared to the soil under shrubs (SH) and grassland (GL), respectively (Table 1). The mean monthly MBC content under grassland (GL) cover ranged from 170.14 ± 1.92 to 230.27 ± 0.71 mg kg^{-1}, which was higher than the MBC content under the other two cover types. This difference was most pronounced in park type(P), where the MBC was, on average, higher by 31.03 and 29.68 mg kg^{-1}compared to shrubs (SH) and forest stand (FS), In the residential area (Ra) type, however, the difference was negligible. Soil C pools varied more among green space types than among vegetation cover types (Table 2). Overall (Table 2), compared to the park type (P), the monthly mean MBC content in the other two green space types decreased by 6.41% and 19.43% ($p < 0.05$), respectively, and WSOC decreased by 7.20% and 15.77% ($p < 0.05$), respectively (Table 2).

The seasonal activity patterns of soil N pools followed a trend similar to those of soil C pools (Table 1; Figure 4). The concentrations of MBN, NH_4^+-N, and NO_3^--N exhibited significant variability across different vegetation covers, particularly for NO_3^--N, which showed a monthly mean value ranging from 12.06 to 5.21 mg kg^{-1} among the three vegetation covers. The variability was even greater across the three green space types (Table 2). In the park type (P), the monthly mean MBN of the grassland (GL) was 30.05 ± 6.0 mg kg^{-1}, representing a significant increase of 23.8% and 26.6% ($p < 0.05$) compared to the other cover types, as well as between shrub (SH) and forest stand (FS) cover soils in residential area (Ra) and street(S). Monthly mean WSON showed significant differences ($p < 0.05$) only between different vegetation covers in park type (P). Overall, differences in soil N pool activity were relatively small among vegetation covers (Table 2). Specifically, NO_3^--N content decreased by 21.71% and 34.5% in the residential area (Ra) and street (S) soils compared to those under the park type (P); NH_4^+-N content decreased by 19.96% and 26.8%, respectively (Figure 4b); and WSON content decreased by 15.19% and 22.83%, respectively, with significant differences ($p < 0.05$) (Table 2). These variations were more pronounced than those observed across different vegetation cover types. Same with soil C pool, the HLM

10.3389/fenvs.2025.1555628

TABLE 2 Differences (mean ± standard deviation) in soil environmental factors under different vegetation cover types, with the interaction being greenspace type and vegetation cover type.

Soil environmental factors	Green space type		Cover type		Interaction
	Mean value		Mean value		P
Soil moisture (%)	P	23 ± 7.8a	SH	22.74 ± 6.45a	0.762
	Ra	21.5 ± 0.0078a	GL	23.2 ± 2.484a	
	S	23.65 ± 2.079a	FS	22.45 ± 1.47a	
pH	P	6.80 ± 0.17a	SH	6.11 ± 0.57a	0****
	Ra	5.72 ± 0.06b	GL	6.23 ± 0.65a	
	S	5.85 ± 0.09b	FS	6.03 ± 0.65a	
Soil temperature (°C)	P	16.14 ± 0.376c	SH	17.16 ± 1.13b	0.017**
	Ra	18.47 ± 1.20a	GL	18.49 ± 1.69a	
	S	18.02 ± 0.94b	FS	16.98 ± 0.92c	
WSOC ($mg{\cdot}kg^{-1}$)	P	170.33 ± 17.53a	SH	189.69 ± 19.44b	0.863
	Ra	158.02 ± 10.79b	GL	201.14 ± 30.10a	
	S	143.45 ± 1.65c	FS	184.95 ± 15.20b	
WSON ($mg{\cdot}kg^{-1}$)	P	19.09 ± 1.45a	SH	15.77 ± 1.45b	0.207
	Ra	16.19 ± 0.86b	GL	17.30 ± 2.63a	
	S	14.73 ± 0.11b	FS	16.92 ± 2.63a	
NH_4^+-N ($mg{\cdot}kg^{-1}$)	P	11.57 ± 0.61a	SH	9.10 ± 2.04a	0.571
	Ra	9.06 ± 0.46b	GL	10.45 ± 1.59a	
	S	8.46 ± 1.16b	FS	9.54 ± 1.59a	
NO_3^--N ($mg{\cdot}kg^{-1}$)	P	10.24 ± 1.58a	SH	6.68 ± 2.13a	0.202
	Ra	8.02 ± 2.01b	GL	9.73 ± 2.14a	
	S	6.57 ± 1.32b	FS	8.42 ± 1.55a	
MBC ($mg{\cdot}kg^{-1}$)	P	210.03 ± 2.41a	SH	155.70 ± 12.60a	0.185
	Ra	196.528 ± 1.53b	GL	157.43 ± 13.34a	
	S	169.22 ± 1.59b	FS	158.6791 ± 11.74a	
MBN ($mg{\cdot}kg^{-1}$)	P	24.94 ± 4.43a	SH	23.93 ± 1.07a	0.18
	Ra	26.60 ± 2.06a	GL	26.578 ± 3.82a	
	S	23.64 ± 1.15a	FS	24.68 ± 3.24a	
CH_4 uptake ($\mu g\ m^{-2}h^{-1}$)	P	43.26 ± 2.47a	SH	42.75 ± 1.07b	0.890
	Ra	42.14 ± 2.13a	GL	44.03 ± 1.34a	
	S	42.00 ± 1.76a	FS	40.63 ± 0.92b	
N_2O emission ($\mu g\ m^{-2}h^{-1}$)	P	71.33 ± 4.05a	SH	62.00 ± 6.78a	0.026*
	Ra	59.48 ± 6.85b	GL	67.24 ± 8.28a	
	S	55.34 ± 5.00b	FS	56.91 ± 8.01a	
CO_2 emission ($mg\ m^{-2}h^{-1}$)	P	415.57 ± 30.16a	SH	373.88 ± 35.92b	0.263
	Ra	377.91 ± 30.16b	GL	418.86 ± 38.52a	
	S	347.53 ± 20.21b	FS	358.26 ± 28.03b	

*Represents level of significance ($p < 0.05$).

TABLE 3 The carbon sequestration of different carbon pools (Mg CO_2-eq ha^{-1}) under different vegetation cover of UGS.

UGS	Treatment	Cumulative soil CO_2 emission	Cumulative soil N_2O emission	Cumulative soil CH_4 uptake	Total GHG emissions	ΔSOC	Annual carbon sequestration of soil SOC
Park	SH	36.33 ± 0.59b	1.85 ± 0.04b	0.09 ± 0.002b	38.05 ± 0.63b	39.45 ± 0.58c	1.39 ± 0.05c
	GL	39.37 ± 0.52a	1.98 ± 0.03a	0.10 ± 0.001a	41.26 ± 0.51a	42.97 ± 0.49a	1.70 ± 0.03b
	FS	34.08 ± 0.16c	1.79 ± 0.04b	0.08 ± 0.001b	35.78 ± 0.20c	37.96 ± 0.24b	2.17 ± 0.04a
Residential area	SH	32.37 ± 0.33b	1.56 ± 0.03b	0.09 ± 0.001a	33.84 ± 0.33b	35.04 ± 0.36b	1.20 ± 0.03b
	GL	36.04 ± 0.23a	1.73 ± 0.04a	0.09 ± 0.001a	37.69 ± 0.24a	39.18 ± 0.16a	1.49 ± 0.07b
	FS	31.41 ± 0.32b	1.37 ± 0.05b	0.08 ± 0.002b	32.70 ± 0.27b	34.58 ± 0.32b	1.88 ± 0.05a
Street	SH	30.07 ± 0.88b	1.48 ± 0.03a	0.09 ± 0.001a	31.47 ± 0.08b	32.10 ± 0.87b	0.63 ± 0.08b
	GL	32.59 ± 0.16a	1.55 ± 0.06a	0.09 ± 0.001a	34.06 ± 0.21a	34.89 ± 0.20a	0.83 ± 005b
	FS	29.15 ± 0.11b	1.30 ± 0.002b	0.09 ± 0.001a	30.36 ± 0.13b	31.85 ± 0.21b	1.48 ± 0.12a

Notes: Lowercase letters in the same horizontal line indicate a significance difference test (LSD), which is statistically significant ($p < 0.05$, $n = 3$).

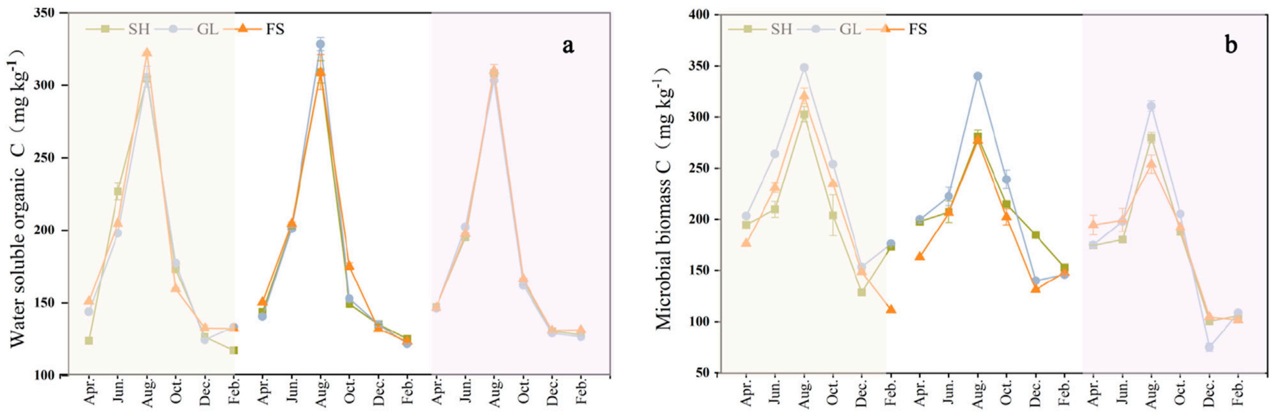

FIGURE 3
Monthly changes of soil C environmental factors under different types of greenspace covered by vegetation. Water soluble organic C (**a**) and soil Microbial biomass C (**b**). These values represent means ± SDs ($n = 3$).

showed that the interaction between green space type and vegetation cover type did not significantly affect the soil N pool (Table 2).

3.2 Impacts of various types of urban vegetation-covered green spaces on soil greenhouse gas fluxes

During the 12-month field observation, soil CO_2 emissions exhibited a clear seasonal pattern under the three vegetation cover types, peaking in summer (June to August) and reaching a minimum in winter (December to February). Summer emissions accounted for 35.86%–38.55% of the annual total, while winter emissions ranged from 12.38% to 15.39% (Figures 5a, b). Among the three green space types, soil CO_2 emissions under grassland (GL) cover were consistently higher than those under the other two vegetation covers, particularly in parks(P), representing a substantial portion of the annual emissions, ranging from 35.86% to 38.55%. In parks, grassland (GL) cover contributed 13.43% more to the monthly emissions than forest stand (FS) cover, leading to a 15.55% increase in annual emissions ($p < 0.05$). Significant differences ($p < 0.05$) in average monthly CO_2 emissions were also observed between shrubs (SH) and forest stand (FS) covers in park (P) green spaces.

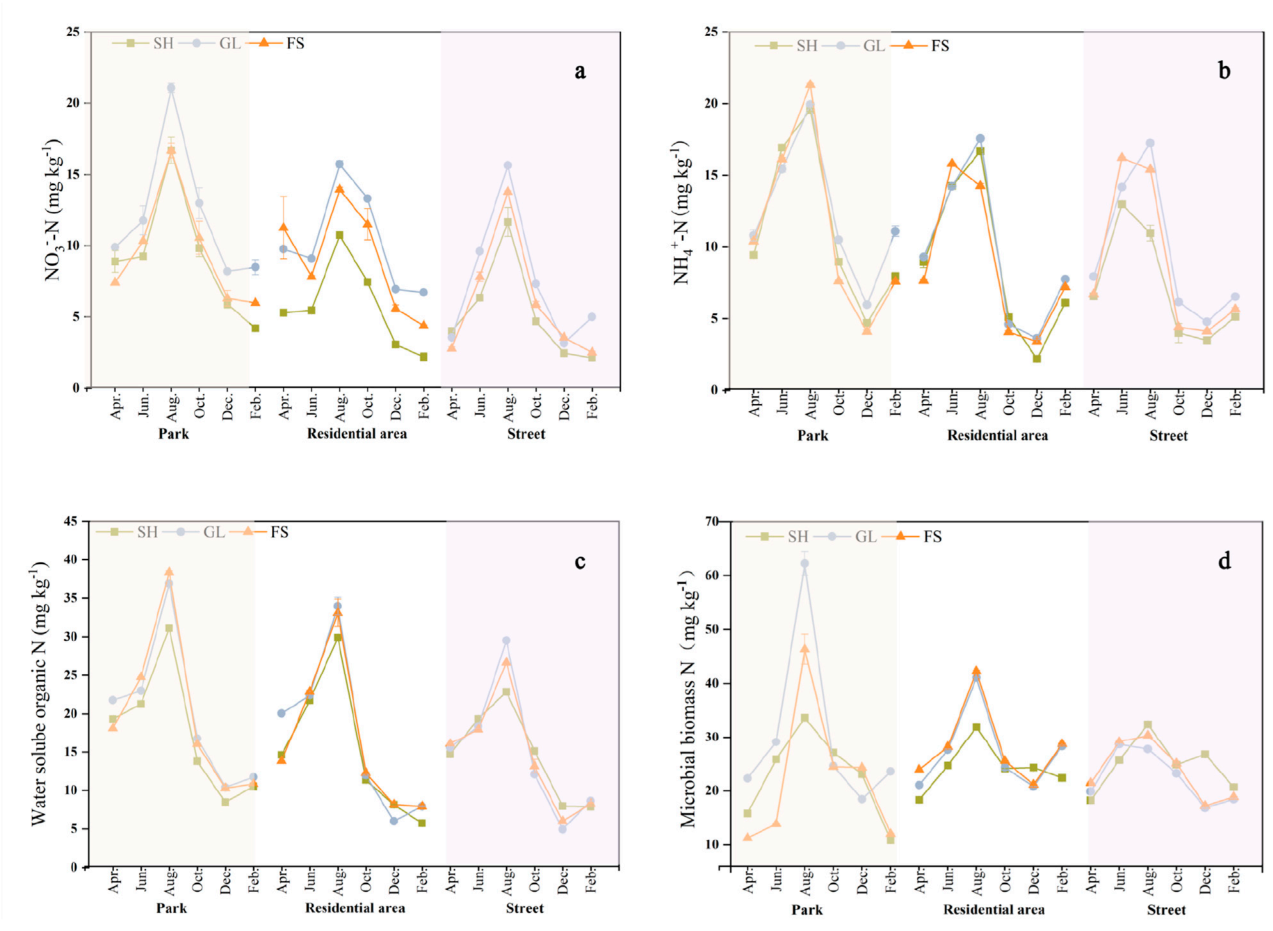

FIGURE 4
Monthly changes of soil N environmental factors under different types of greenspace covered by vegetation. NO_3^--H (**a**), NH_4^+-N (**b**), water - soluble organic N (**c**), and microbial biomass N (**d**). These values represent means ± SDs (n = 3).

The N_2O emission pattern followed a similar trend to CO_2 emissions, with GL > SH > FS observed across all green space types (Figures 5c, d). Grassland (GL) cover exhibited 11.11% higher N_2O emissions in P-type green spaces compared to forest stand (FS) cover. Significant differences in N_2O emissions were also noted between shrubs (SH) and forest stand (FS) soils in the residential area (Ra) ($p < 0.05$). In general, the emission patterns for CO_2 and N_2O mirrored each other across vegetation covers and green space types. Notably, CO_2 emissions exhibited significant differences between both green space types and vegetation cover types, while N_2O emissions showed significant variation only between green space types ($p < 0.05$). The HLM revealed that the interaction between green space type and vegetation cover was statistically significant only for N_2O fluxes ($p < 0.05$) (Table 1).

Soils from various green space types, characterized by different vegetation covers, acted as sinks for CH_4 (Figure 5e). While CH_4 emissions showed no clear seasonal pattern, CH_4 uptake was notably higher in summer (Figure 5f). The average CH_4 uptake by loam soil beneath the three vegetation cover types ranged from 41.55 ± 1.36 to 443.69 ± 0.82 μg m^{-2}h^{-1}. The park grassland (P-GL) and the forest stand in the residential area (Ra-FS) average CH_4 uptake was significantly higher (39.71 ± 0.74 and 45.51 ± 1.23 μg m^{-2}h^{-1}) compared to the other vegetation-covered soils in the same green space type ($p < 0.05$). Overall, the CH_4 uptake by grassland (GL) cover was statistically distinguished from the other two vegetation covered soils in the same green space type ($p < 0.05$). Same to soil CO_2 emissions, the HLM showed that the interaction between green space type and vegetation cover type did not significantly affect the soil CH_4 uptake (Table 2).

3.3 Effects of soil environmental factors on soil GHG emissions

All PC1 accounted for 62.7% of the variance, which was greater than PC2. The analysis revealed a significant positive correlation between soil carbon and nitrogen pools across the greenfield soils of all vegetation cover types. However, the correlation between pH and soil water content, soil carbon and nitrogen pools was weaker. The differences between greenfield types were significantly greater than those under different vegetation cover types, indicating stronger differences between groups (Figures 7a,b).

Random forest modeling results showed that for CO_2 fluxes, WSOC under the three vegetation cover types was significantly

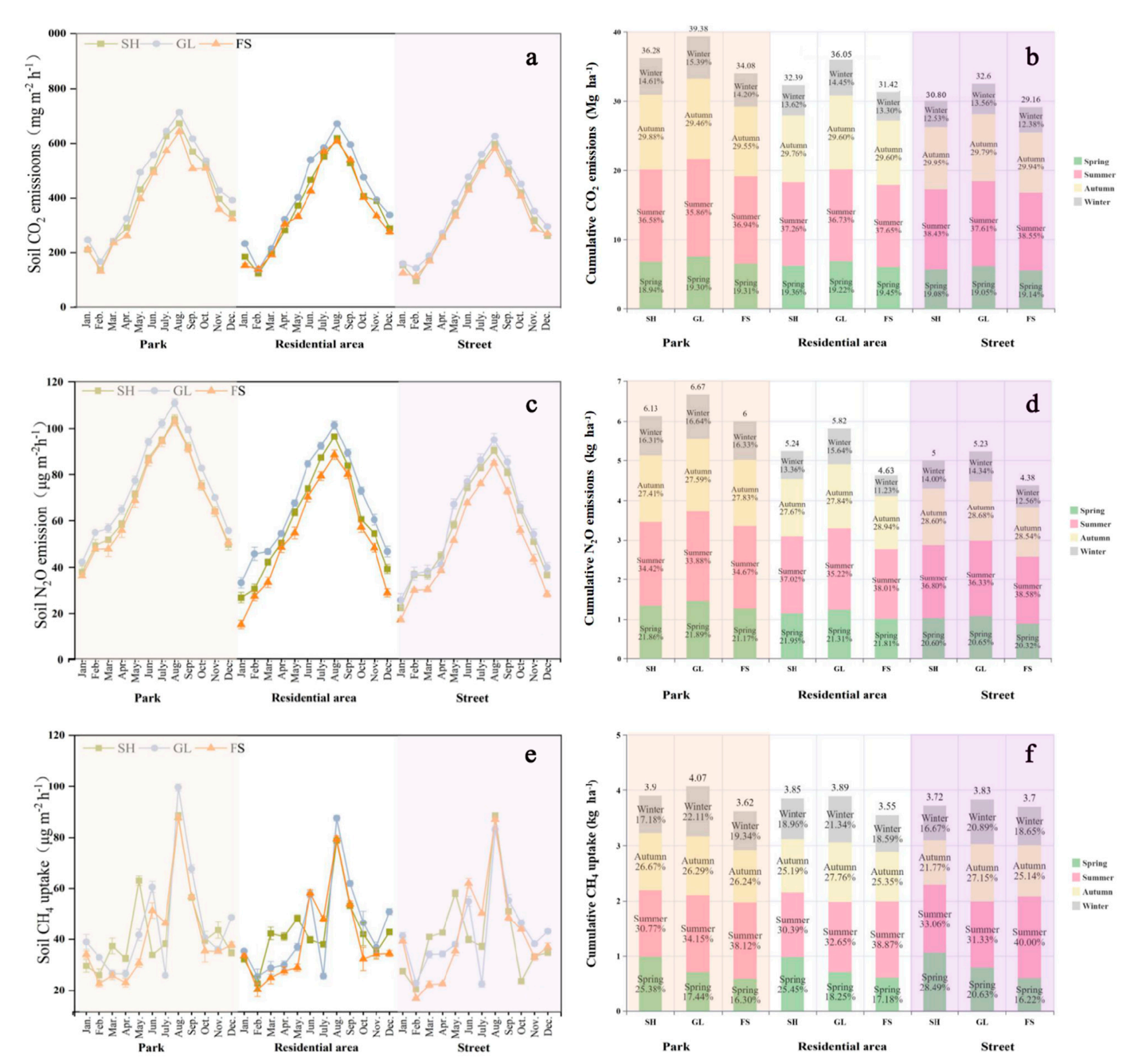

FIGURE 5
Monthly mean ± standard deviation (n = 3) under different urban vegetation cover and green space types: **(a)** soil CO_2 emission flux, **(c)** soil N_2O emission flux, **(e)** soil CH_4 uptake flux, errors are represented by error bars; **(b)** soil cumulative CO_2 emissions, **(d)** soil cumulative N_2O emissions, and **(f)** soil cumulative CH_4 uptake. The four colors in the column represent the proportions of greenhouse gas fluxes in different seasons to the annual greenhouse gas flux, with spring, summer, autumn, and winter corresponding to March-May, June-August, September-November, and December-February respectively.

correlated with soil temperature (Supplementary Figures S2a, d, g), with a significance level greater than 20% in shrubs (SH), which was highly similar to the results of the random forest analysis under different green space types (Supplementary Figures S1a, d, g). For N_2O fluxes, the importance of WSON activity on N_2O fluxes was greater than 20% for all three vegetation types under cover, and 51% in shrubs (SH), which was statistically significant (Supplementary Figure S2b). In addition, NH_4^+-N was second only to WSON on N_2O fluxes in shrubs (SH) and grassland (GL), but had a minimal influence on N_2O in forest stand (FS). Similarly, the results of random forests under different green space types showed that WSON had an effect of greater than 20% on N_2O fluxes in both park (P) and residential area (Ra), and NH_4^+-N also had a significant effect on N_2O fluxes in all three green space types, especially in residential area (Ra), with a 29% effect. Except for patchy forest stand (FS) cover soil, pH showed significant importance in CH_4 uptake under both vegetation types, which was similar to the results of the random forest analysis under the three green space types, but its lowest importance was observed in forest stand (FS) (Supplementary Figure S2i).

The RDA1s of the redundancy analyses for different vegetation covers and green space types were all greater than 60%, substantially exceeding the RDA2s (Figures 7a–f). The results indicated that the effects of soil CN pool activities on GHG fluxes were relatively

 10.3389/fenvs.2025.1555628

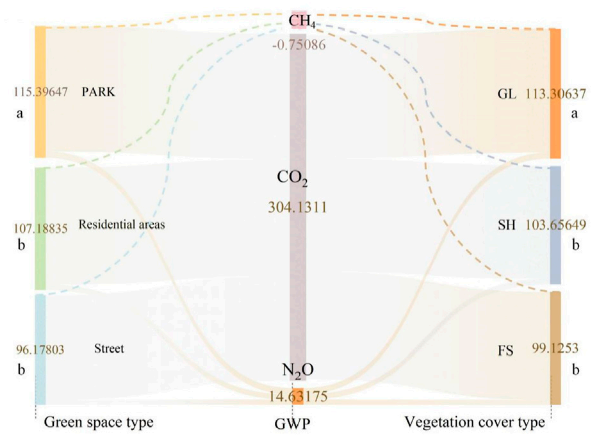

FIGURE 6
After converting the GHG fluxes of different vegetation coverage green space types into GWP coefficients, a Sankey diagram is used to represent the contribution of different treatments to GWP under different coverage types. The columns of different colors on both sides represent different vegetation coverage and green space. The total GWP of the type. The middle column shows the total GWP of all vegetation cover and green space types. The larger the GWP value, the longer the column. The width of the connection between columns reflects the contribution to GWP. The dashed line indicates that CH_4 absorption reduces the GWP value. Letters next to the bars indicate significant differences between treatments determined by the least significant difference (LSD) test with $p < 0.05$.

consistent under different vegetation cover types. Specifically, the soil CN pool activities were positively correlated with CO_2 and N_2O emissions, while CH_4 fluxes demonstrated a weaker correlation with the soil CN pools. Additionally, WSOC had a strong positive correlation with CO_2 fluxes across all three vegetation covers (Figures 7d–f). For N_2O fluxes, NH_4^+-N and WSON exhibited strong correlations, although WSON showed a weaker correlation in grassland. In contrast, CH_4 and soil physicochemical properties did not exhibit a strong correlation with carbon and nitrogen pool activities. The RDA analysis results of the three green space types were similar to those of the vegetation cover types (Figures 7a–c).

3.4 Responses of soil carbon sequestration to different urban vegetation cover and green space types

Our results indicate that the soils under the three vegetation covers exhibited varying levels of soil carbon sequestration, with forest stand (FS) exhibiting the highest sequestration, followed by grassland (GL) and shrubs (SH). However, the level of variability differed among the various green space types (Figure 8). Specifically, for the park type (P), the carbon sequestration of forest stand (FS) soil was 2.17 ± 0.04 Mg CO_2 eq $ha^{-1}yr^{-1}$,which represents increases of 35.94% and 21.65% compared to the soil under the grassland (GL) and shrubs (SH). This difference was highly significant ($p < 0.001$). Additionally, soil carbon sequestration in the park green space (P) was 1.75 ± 0.18 Mg CO_2 eq $ha^{-1}yr^{-1}$, which was significantly higher than the other two green space types by 15.13% and 78.57%, respectively. This difference was statistically significant ($p < 0.05$).

4 Discussion

4.1 Response of soil GHG flux to changes in vegetation cover green space types

Carbon dioxide, being one of the pivotal greenhouse gases, accounts for approximately 60% of the contribution to global warming, as reported (Kaye et al., 2005). In our study, regardless of the green space type, the CO_2 flux was the primary source of greenhouse gas emissions, consistent with the findings of Wu et al. (2019). In conjunction with the alterations in soil environmental factors induced by variations in green space types, the present study ascertained that the CO_2 in urban green spaces predominantly hinged on the activity of WSOC.

WSOC, an essential component of soil organic carbon pools, can alter the hygroscopic characteristics of aerosols, thus influencing CO_2 emissions, as documented in (Yang et al., 2017), higher soil temperatures in grassland accelerate the decomposition rate of soil organic carbon (Xu et al., 2021), and the increased bioavailability of WSOC enhances the growth and activity of soil microorganisms. This promotes the decomposition of soil organic matter and the emission of soil CO_2, in line with Zhang's findings (Figure 3a) (Zhang et al., 2015), Moreover, the three vegetation covers were within the more suitable pH range for the park type under high-intensity management. This suggests that the green space type influences the intensity of soil exposure to management and disturbance (Hao et al., 2017). Activities like watering and fertilizing enhance the dissolution and movement of nutrients and WSOC in the soil surface layer, creating an optimal environment for the dissolution and transfer of nutrients and WSOC. Another possible explanation is that human disturbances lead to non-equilibrium dynamics, reducing microbial interspecific competition, as outlined in the mediated disturbance hypothesis. This, in turn, increases microbial populations in the soil, which indirectly raises CO_2 emissions through microbial heterotrophic respiration and the decomposition of soil organic matter (SOM).

Soil nitrification and nitrogen mineralization are important pathways for soil N_2O production (Martínez-Espinosa et al., 2021). Microbial production and consumption of N_2O are influenced by both the physical and chemical characteristics of the soil and the soil management practices. The presence of grassland encourages human activities such as walking, exercising, and picnicking, these activities lead to increased soil compaction, which creates an anaerobic soil environment. Under anaerobic conditions, NO_3^--N serves as an electron acceptor and is gradually reduced to N_2O through the catalytic action of various enzymes (Table 1). In parks with well-managed soil and fertilizer application, fertilizers dissolved into the soil, primarily existing as ammonium ions or inorganic nitrogen. This process provides essential substrates for nitrification and nitrogen mineralization (Table 1), ultimately increasing N_2O emissions (Martínez-Espinosa et al., 2021).

Soil CH_4 flux results from the balance between CH_4 production and oxidation processes. The extent of soil CH_4 production and

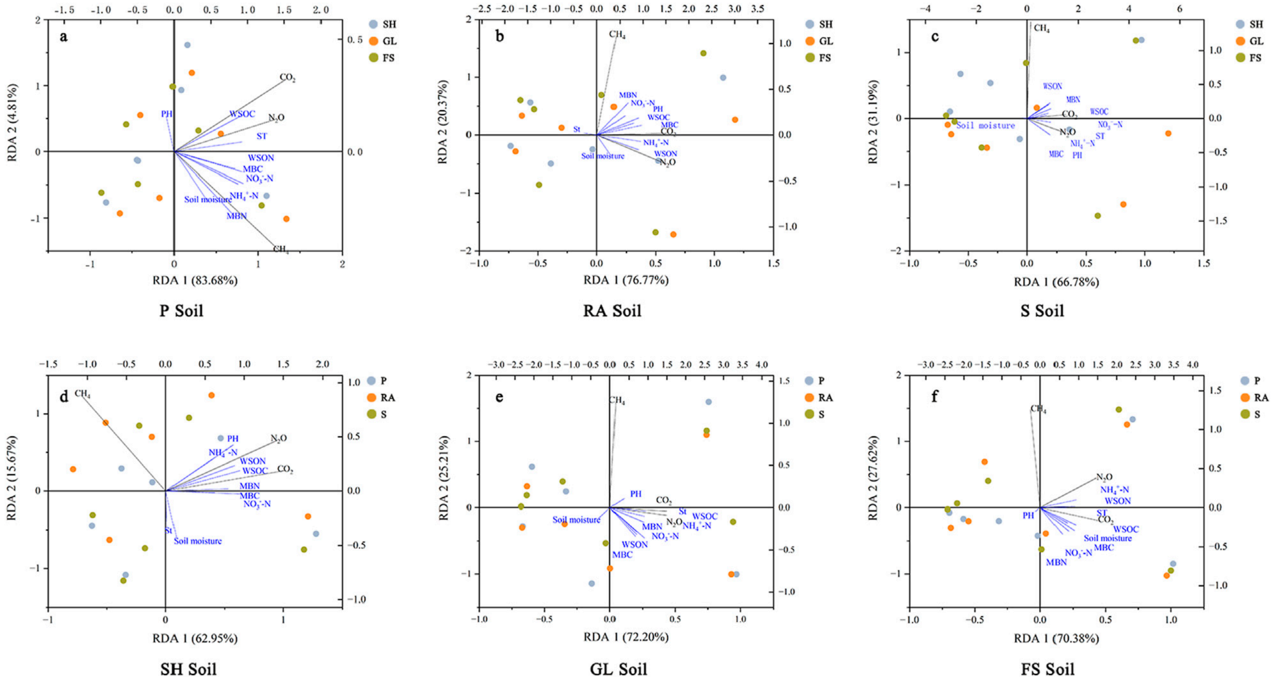

FIGURE 7
Redundancy analysis to investigate the impact of soil environmental factors on GHG fluxes in different types of vegetation cover **(a–c)** and green space types **(d–f)**.

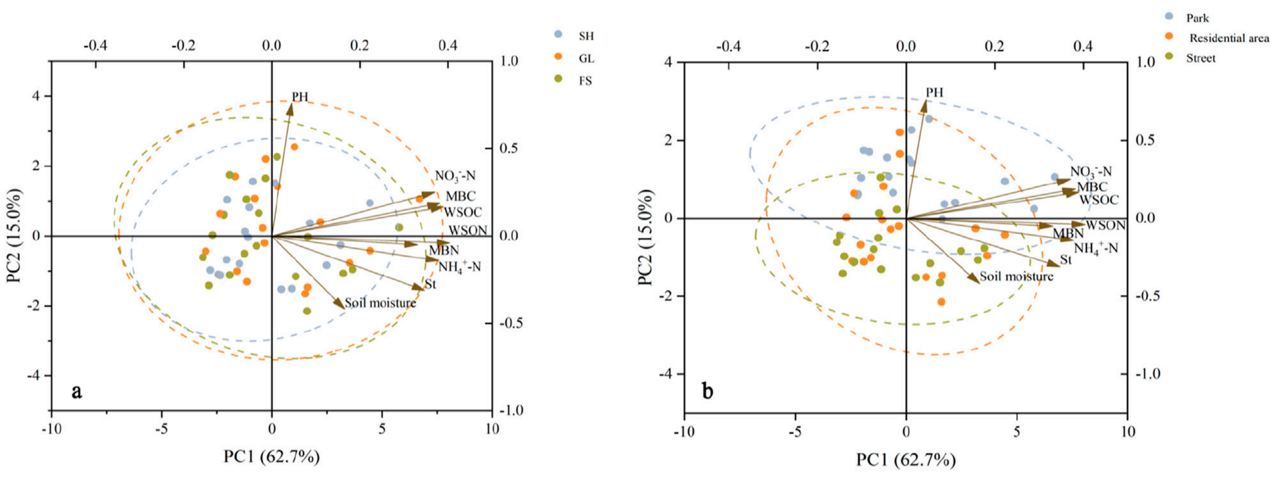

FIGURE 8
Principal component analysis of soil physical and chemical properties under different vegetation cover **(a)** and green space types **(b)**.

consumption determines whether the soil acts as a source or a sink of CH_4. In diverse green spaces and vegetation types, the soil exhibits the propensity for CH_4 absorption and thus serves as a sink of CH_4. Alterations in soil pH can influence methane uptake by modulating the balance between CH_4 production and oxidation. Due to the high root activity of grassland, alkaline substances such as carbonates are secreted, neutralizing acidic components of the soil and raising the pH. Soils with high salt content enhance the effectiveness of soil K^+, which inhibits CH_4 oxidation by altering the interactions between NH_4^+-N and clay particles. In park green spaces, the long-term use of calcium and magnesium fertilizers to neutralize soil acidity, combined with human trampling, prevents oxygen from entering the surface soil, thus slowing down the CH_4 oxidation process (Tong et al., 2012) (Supplementary Figure S1, S2).

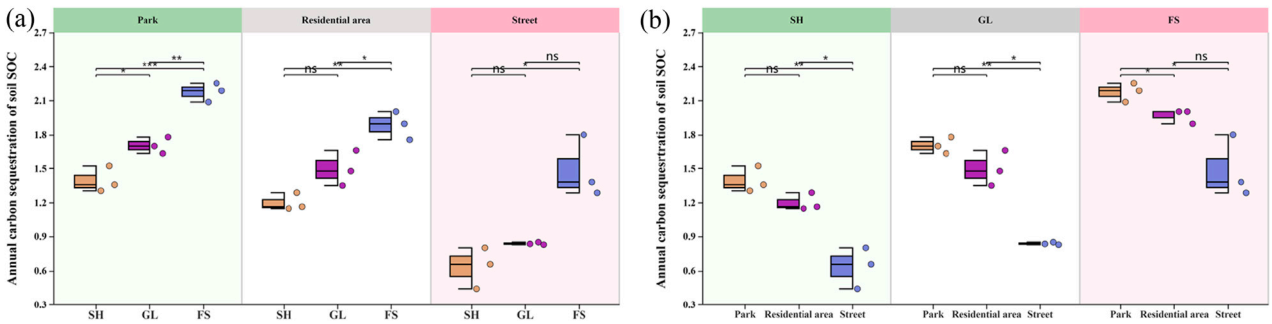

FIGURE 9
The differences in soil carbon sequestration with across to different vegetation coverage **(a)** and green space types **(b)** were illustrated using box plots. In these plots, the horizontal line in side the box signifies the mean value. While upper and lower whiskers denote box plot denote the maximum and minimum values of the data, respectively, he upper and lower edges of the box correspond to the upper and lower quartiles. The upper connecting line was uesd to indicate the comparison groups. A symbol "*" denotes a significant difference among the four treatments (P < 0.05), and 'ns' implies no significant difference between the two.

4.2 Effects of different types of green space covered by urban vegetation on soil carbon sequestration

Soil SOC content is widely used as the primary indicator of soil carbon sequestration capacity (Koorneef et al., 2024). In this study, we found that different vegetation cover types and green space categories significantly affected soil carbon sequestration, with the highest carbon sequestration observed under forest cover and the lowest under grassland. Our findings align with the findings of Livesley et al. (Weissert et al., 2016), as the accumulation and rapid decomposition of apoplastic materials beneath forest cover, due to the shedding of tree leaves, likely serves as the primary source of soil organic carbon. During the fall season, the decomposition of these materials not only improves the physicochemical properties of the soil but also increases its carbon content. Meanwhile, the reduced SOC sequestration observed in grassland and shrub cover is presumably attributed to the limited fall materials input and high plant density. An increase in plant density results in overlapping canopies, which inhibits microbial activity and intensifies competition among root systems, ultimately affecting soil carbon sequestration capacity (Figure 9a).

Unlike residential or street green spaces, which primarily serve individual households, park green spaces are regional ecosystems that play a critical role in air purification and provide a range of ecosystem services. Parks green spaces are more integrated, and the ecological cycling process within their soil may be more resilient to the adverse impact of urban air pollution and water quality degradation. As a result, parks tend to have higher carbon sequestration capacity. Another plausible explanation for this difference is the diverse vegetation in park types, which contributes significantly to the increase in soil SOC (Supplementary Table S1). Increased plant biodiversity enhances carbon inputs from the root to the microbial community, boosting soil overall soil carbon storage capacity (Lange et al., 2015). In residential areas or street green spaces, human activities are more prevalent, which may influence soil carbon sequestration in various ways. The lower soil carbon sequestration observed in street green spaces is likely due to their proximity to traffic arteries. The increase in automobile traffic flow has led to an elevation in vehicle emissions, including harmful gases such as sulfur dioxide (SO_2), nitrogen oxides, and particulate matter. These pollutant gases may infiltrate the soil through deposition, reducing microbial and root activity, and subsequently lowering the soil's carbon sequestration capacity (Ahmad et al., 2021) (Figure 9b).

4.3 Urban soil management under the perspective of carbon neutrality: how to maximize the urban soil carbon sequestration function?

Our findings indicate that urban green space, as a semi-natural ecosystem with both natural ecological functions and human intervention characteristics, experiences an impact on its soil carbon sequestration function from functional pathways Consequently, human intervention in soil management practices to reduce soil greenhouse gas emissions is an effective approach to enhancing the carbon sequestration function of soils (Zhang J. et al., 2024).

Our study demonstrates that WSOC is a significant factor influencing CO_2 emissions across various vegetation cover types and green space categories. Therefore, reducing the decomposition rate of WSOC may lead to a reduction in CO_2 flux. Although the decomposition of WSOC is accelerated in grassland due to higher soil temperatures, the relatively low microbial abundance in these areas provides a potential means of mitigating CO_2 flux (Smith et al., 2015). Furthermore, leaching plays a critical role in converting SOC to WSOC. Therefore, minimizing soil disturbance in green space management practices and employing appropriate irrigation techniques and frequencies can control the conversion of SOC to WSOC and enhance the stability of the soil carbon pool (Arce et al., 2021).

Currently, nitrification inhibitors such as dicyandiamide and thiourea have emerged as an effective strategy for mitigating soil nitrification processes (Guo et al., 2022). These inhibitors work by reducing the activity of ammonia-oxidizing bacteria, thereby slowing down the conversion of NH_4^+-N to NO_3^--N and reducing soil N_2O emissions. However, it is important to note that the use of nitrification inhibitors can affect the structure of soil microbial communities, which in turn impacts both the carbon and nitrogen cycles within the soil ecosystem. This has been supported by research conducted by SHU et al. (Section and Sciences, 2017), Additionally, maintaining moderate soil moisture and avoiding excessive irrigation, which can lead to poor soil aeration and inhibit nitrification, represent another effective approach (Lan et al., 2013).

Our findings also suggest that a more neutral soil pH enhances CH_4 absorption, although this difference is not statistically significant. Furthermore, soil pH regulation is a key factor not only in CH_4 absorption but also in the broader context of soil carbon and nitrogen cycles, as it influences plant growth and microbial activity. Common soil pH modifiers such as calcium carbonate and ferrous sulfate, which are suitable for acidic and alkaline soils respectively, increase the availability of K^+ and consequently inhibit CH_4 oxidation (Nikolaisen et al., 2023).

It is worth mentioning that fertilization can rapidly replenish the soil SOC content, enhance the structure of soil aggregates, and reduce the decomposition and loss of organic carbon. Fertilization plays a crucial role in increasing and stabilizing the SOC content in the soil (Liu C. et al., 2024). As a result, it has emerged as another viable method to enhance the soil carbon sequestration function. However, urban pollution has become a significant factor affecting the carbon sequestration potential of urban green space soils. Thus, it is equally crucial to increase the accumulation of organic carbon while improving the resistance of urban soils to external disturbances. Biochar-based fertilizers, which combine the advantages of traditional fertilizers with biochar, have proven effective in improving soil structure, adsorbing pollutants, increasing vegetation productivity, and enhancing soil carbon sequestration capacity. These properties make biochar-based fertilizers an ideal solution for boosting the carbon sequestration capacity and stress tolerance of urban soils (Shiu et al., 2022).

5 Limitations of the study

This study has certain limitations. Firstly, data collection was confined to the southeastern coastal regions of China, which could affect the applicability of our conclusions to other areas. Also, the sample area and soil depth may limit the generalizability of our findings. Our analysis of soil carbon sinks excluded deeper soil layers (beyond 50 cm), but the root systems of grassland are primarily concentrated in the topsoil (Wei et al., 2018). While root exudates can help stabilize surface SOC through adhesion, the lack of such biological activities in deeper soil layers may lead to an overestimation of soil SOC content under grassland cover. This potential deviation is not fully addressed in our model (Chen J. et al., 2022). Lastly, soil carbon sequestration is a gradual, long-term process. Long-term monitoring is essential to better understand how soil greenhouse gas emissions and carbon sequestration may respond to different green space types and vegetation coverages.

6 Conclusion

In this study, we investigated the variations in soil greenhouse gas fluxes and soil carbon sequestration capacity across different green space types with varying vegetation coverage. The results demonstrate that changes in the types of green space and the vegetation type significantly influence soil SOC accumulation and carbon sequestration function. Forest cover and park green spaces exhibit the most effective soil carbon sequestration functions. From an ecological and environmental perspective, urban construction should integrate management strategies, such as the application of soil conditioners or fertilization, to mitigate greenhouse gas emissions or enhance SOC accumulation. Moreover, it is necessary to incorporate these management approaches into the overall assessment of urban green space carbon sequestration capability, which will contribute to maintaining the balance of the urban ecosystem.

Data availability statement

The original contributions presented in the study are included in the article/Supplementary Material, further inquiries can be directed to the corresponding author.

Author contributions

RZ: Conceptualization, Formal Analysis, Investigation, Project administration, Supervision, Writing – review and editing, Data curation, Methodology, Software, Validation, Visualization, Writing – original draft. XC: Methodology, Supervision, Visualization, Writing – review and editing. WC: Methodology, Writing – review and editing, Project administration, Resources. FL: Supervision, Validation, Visualization, Writing – review and editing. SL: Supervision, Formal Analysis, Investigation, Methodology, Writing – review and editing. HS: Formal Analysis, Investigation, Methodology, Project administration, Validation, Visualization, Writing – review and editing. ZN: Investigation, Software, Writing – review and editing. YC: Validation, Visualization, Writing – review and editing. DL: Project administration, Resources, Supervision, Writing – review and editing. YZ: Supervision, Writing – review and editing. YS: Project administration, Resources, Supervision, Conceptualization, Formal Analysis, Funding acquisition, Investigation, Writing – original draft, Writing – review and editing.

Funding

The author(s) declare that financial support was received for the research and/or publication of this article. This research was funded by the Key Research and Development Program of Zhejiang Province (Grant Nos. 2023C02003; 2021C02005), This research was also funded by the National Natural Science Foundation of China (Grant Nos. 32001315; U1809208; 31870618).

Acknowledgments

We would like to thank the editor and reviewers for their contributions to the peer-review process of our study.

Conflict of interest

The authors declare that the research was conducted in the absence of any commercial or financial relationships that could be construed as a potential conflict of interest.

Generative AI statement

The author(s) declare that no Generative AI was used in the creation of this manuscript.

Supplementary material

The Supplementary Material for this article can be found online at: https://www.frontiersin.org/articles/10.3389/fenvs.2025.1555628/full#supplementary-material

References

Ahmad, T., Ahmad, K., Khan, Z. I., Munir, Z., Khalofah, A., Al-Qthanin, R. N., et al. (2021). Chromium accumulation in soil, water and forage samples in automobile emission area. *Saudi J. Biol. Sci.* 28, 3517–3522. doi:10.1016/j.sjbs.2021.03.020

Aram, F., Higueras García, E., Solgi, E., and Mansournia, S. (2019). Urban green space cooling effect in cities. *Heliyon* 5, e01339. doi:10.1016/j.heliyon.2019.e01339

Aramburu Merlos, F., Silva, J. V., Baudron, F., and Hijmans, R. J. (2023). Estimating lime requirements for tropical soils: model comparison and development. *Geoderma* 432, 116421–116422. doi:10.1016/j.geoderma.2023.116421

Arce, M. I., Bengtsson, M. M., von Schiller, D., Zak, D., Täumer, J., Urich, T., et al. (2021). Desiccation time and rainfall control gaseous carbon fluxes in an intermittent stream. *Biogeochemistry* 155, 381–400. doi:10.1007/s10533-021-00831-6

Aronson, M. F. J., Lepczyk, C. A., Evans, K. L., Goddard, M. A., Lerman, S. B., MacIvor, J. S., et al. (2017). Biodiversity in the city: key challenges for urban green space management. *Front. Ecol. Environ.* 15, 189–196. doi:10.1002/fee.1480

Chaurasia, M., Patel, K., and Rao, K. S. (2023). Impact of anthropogenic land uses on soil microbiological activity in a peri-urban landscape. *Environ. Monit. Assess.* 195, 1–22. doi:10.1007/s10661-023-11822-5

Chen, J., Cui, H. Y., Jia, B., Gang, S., Li, Y., Li, F. C., et al. (2022a). Soil sampling depth matters in assessing the impact of shrubification on soil organic carbon storage in grazed alpine meadows. *Geoderma* 426, 116119. doi:10.1016/j.geoderma.2022.116119

Chen, X., Zhang, X., Liu, M., Xu, Z., and Wei, H. (2022b). Urbanization induced changes in the accumulation mode of organic carbon in the surface soil of subtropical forests. *Catena* 214, 106264. doi:10.1016/j.catena.2022.106264

Churkina, G. (2016). The role of urbanization in the global carbon cycle. *Front. Ecol. Evol.* 3, 1–9. doi:10.3389/fevo.2015.00144

Churkina, G., Brown, D. G., and Keoleian, G. (2010). Carbon stored in human settlements: the conterminous United States. *Glob. Change Biol.* 16, 135–143. doi:10.1111/j.1365-2486.2009.02002.x

Demuzere, M., Orru, K., Heidrich, O., Olazabal, E., Geneletti, D., Orru, H., et al. (2014). Mitigating and adapting to climate change: multi-functional and multi-scale assessment of green urban infrastructure. *J. Environ. Manag.* 146, 107–115. doi:10.1016/j.jenvman.2014.07.025

Enescu, R. E., Dincă, L., Zup, M., Davidescu, Ş., and Vasile, D. (2022). Assessment of soil physical and chemical properties among urban and peri-urban forests: a case study from metropolitan area of brasov. *Forests* 13, 1070. doi:10.3390/f13071070

Guo, C., Wang, H., Zou, D., Wang, Y., and Han, X. (2022). A novel amended nitrification inhibitor confers an enhanced suppression role in the nitrification of ammonium in soil. *J. Soils Sediments* 22, 831–843. doi:10.1007/s11368-021-03118-3

Hao, X., You, M., Han, X., Li, H., Zou, W., and Xing, B. (2017). Redistribution of different organic carbon fractions in the soil profile of a typical Chinese mollisol with land-use change. *Commun. Soil Sci. Plant Analysis* 48, 2369–2380. doi:10.1080/00103624.2017.1358741

Kaye, J. P., McCulley, R. L., and Burke, I. C. (2005). Carbon fluxes, nitrogen cycling, and soil microbial communities in adjacent urban, native and agricultural ecosystems. *Glob. Change Biol.* 11, 575–587. doi:10.1111/j.1365-2486.2005.00921.x

Koorneef, G. J., Pulleman, M. M., Comans, R. N., van Rijssel, S. Q., Barré, P., Baudin, F., et al. (2024). Assessing soil functioning: what is the added value of soil organic carbon quality measurements alongside total organic carbon content? *Soil Biol. Biochem.* 196, 109507. doi:10.1016/j.soilbio.2024.109507

Lal, R., and Augustin, B. (2012). Carbon sequestration in urban ecosystems. *Carbon Sequestration Urban Ecosyst.*, 1–385. doi:10.1007/978-94-007-2366-5

Lan, T., Han, Y., Roelcke, M., Nieder, R., and Cai, Z. (2013). Processes leading to N2O and NO emissions from two different Chinese soils under different soil moisture contents. *Plant Soil* 371, 611–627. doi:10.1007/s11104-013-1721-1

Lange, M., Eisenhauer, N., Sierra, C. A., Bessler, H., Engels, C., Griffiths, R. I., et al. (2015). Plant diversity increases soil microbial activity and soil carbon storage. *Nat. Commun.* 6, 6707. doi:10.1038/ncomms7707

Liao, L., Zhao, C., Li, X., and Qin, J. (2021). Towards low carbon development: the role of forest city constructions in China. *Ecol. Indic.* 131, 108199. doi:10.1016/j.ecolind.2021.108199

Liu, C., He, C., Chang, S. X., Chen, X., An, S., Wang, D., et al. (2024a). Fertilization and tillage influence on soil organic carbon fractions: a global meta-analysis. *Catena* 246, 108404. doi:10.1016/j.catena.2024.108404

Liu, K., Xue, Y., Chen, Z., and Miao, Y. (2023). The spatiotemporal evolution and influencing factors of urban green innovation in China. *Sci. Total Environ.* 857, 159426. doi:10.1016/j.scitotenv.2022.159426

Liu, Q., Wang, S., Ma, R., Huang, F., Li, J., Ye, S., et al. (2024b). Comparative analysis of forest soil carbon sink and source based on bibliometrics: development, hotspots, and trends. *J. Clean. Prod.* 480, 144106. doi:10.1016/j.jclepro.2024.144106

Liu, Y., Fan, C., and Xue, D. (2024c). A review of the effects of urban and green space forms on the carbon budget using a landscape sustainability framework. *Sustain. Switz.* 16, 1870–1929. doi:10.3390/su16051870

Lv, M., Gao, W., Li, J., Ye, X., Xu, T., Liu, L., et al. (2022). Identification of zones contaminated with phthalates and polycyclic aromatic hydrocarbons by concentrations in gridded soil with 1/6° latitude by 1/4° longitude resolution: a case study of Zhejiang, China. *J. Soils Sediments* 22, 67–78. doi:10.1007/s11368-021-03075-x

Martínez-Espinosa, C., Sauvage, S., Al Bitar, A., Green, P. A., Vörösmarty, C. J., and Sánchez-Pérez, J. M. (2021). Denitrification in wetlands: a review towards a quantification at global scale. *Sci. Total Environ.* 754, 142398. doi:10.1016/j.scitotenv.2020.142398

Morel, J. L., Chenu, C., and Lorenz, K. (2015). Ecosystem services provided by soils of urban, industrial, traffic, mining, and military areas (SUITMAs). *J. Soils Sediments* 15, 1659–1666. doi:10.1007/s11368-014-0926-0

Nikolaisen, M., Cornulier, T., Hillier, J., Smith, P., Albanito, F., and Nayak, D. (2023). Methane emissions from rice paddies globally: a quantitative statistical review of controlling variables and modelling of emission factors. *J. Clean. Prod.* 409, 137245. doi:10.1016/j.jclepro.2023.137245

Ónodi, G., Kertész, M., Kovács-Láng, E., Ódor, P., Botta-Dukát, Z., Lhotsky, B., et al. (2017). Estimating aboveground herbaceous plant biomass via proxies: the confounding effects of sampling year and precipitation. *Ecol. Indic.* 79, 355–360. doi:10.1016/j.ecolind.2017.04.011

Peaden, S. J. (2019). Classification of urban forms and their relationship with vegetation cover in cache county, Utah.

Reynolds, H. L., Brandt, L., Fischer, B. C., Hardiman, B. S., Moxley, D. J., Sandweiss, E., et al. (2020). Implications of climate change for managing urban green infrastructure: an Indiana, US case study. *Clim. Change* 163, 1967–1984. doi:10.1007/s10584-019-02617-0

Rouge, B., and Patrick, W., Jr (1981). Nitrate reduction to ammonium and organic nitrogen in an estuarine sediment. 13, 279, 283. doi:10.1016/0038-0717(81)90063-8

Rubaiyat, A., Hossain, M. L., Kabir, M. H., Sarker, M. M. H., Salam, M. M. A., and Li, J. (2023). Dynamics of greenhouse gas fluxes and soil physico-chemical properties in agricultural and forest soils. *J. Water Clim. Change* 14, 3791–3809. doi:10.2166/wcc.2023.338

Schetke, S., Qureshi, S., Lautenbach, S., and Kabisch, N. (2016). What determines the use of urban green spaces in highly urbanized areas? - examples from two fast growing Asian cities. *Urban For. Urban Green.* 16, 150–159. doi:10.1016/j.ufug.2016.02.009

Section, S. S., Sciences, A., Mosier, A. R., and Chen, D. (2017). Using nitrification inhibitors to mitigate agricultural N 2 O emission: a double-edged sword. *Glob. Chang. Biol.* 23, 485–489. doi:10.1111/gcb.13338

Serrano-Silva, N., Sarria-Guzmán, Y., Dendooven, L., and Luna-Guido, M. (2014). Methanogenesis and methanotrophy in soil: a review. *Pedosphere* 24, 291–307. doi:10.1016/S1002-0160(14)60016-3

Shiu, J. H., Huang, Y. C., Lu, Z. T., Jien, S. H., Wu, M. L., and Wu, Y. T. (2022). Biochar-based compost affects bacterial community structure and induces a priming effect on soil organic carbon mineralization. *Processes* 10, 682. doi:10.3390/pr10040682

Smith, L. S., Broyles, M. E. J., Larzleer, H. K., and Fellowes, M. D. E. (2015). Adding ecological value to the urban lawnscape. Insect abundance and diversity in grass-free lawns. *Biodivers. Conservation* 24, 47–62. doi:10.1007/s10531-014-0788-1

Song, X., Peng, C., Ciais, P., Li, Q., Xiang, W., Xiao, W., et al. (2020). Nitrogen addition increased CO2 uptake more than non-CO2 greenhouse gases emissions in a Moso bamboo forest. *Sci. Adv.* 6, eaaw5790–10. doi:10.1126/sciadv.aaw5790

Tong, C., Wang, W. Q., Huang, J. F., Gauci, V., Zhang, L. H., and Zeng, C. S. (2012). Invasive alien plants increase CH4 emissions from a subtropical tidal estuarine wetland. *Biogeochemistry* 111, 677–693. doi:10.1007/s10533-012-9712-5

Vasenev, V., and Kuzyakov, Y. (2018). Urban soils as hot spots of anthropogenic carbon accumulation: review of stocks, mechanisms and driving factors. *Land Degrad. Dev.* 29, 1607–1622. doi:10.1002/ldr.2944

Wang, E., Yuan, N., Lv, S., Tang, X., Wang, G., Wu, L., et al. (2022). Biochar-based fertilizer decreased soil N2O emission and increased soil CH4 uptake in a subtropical typical bamboo plantation. *Forests* 13, 2181. doi:10.3390/f13122181

Wang, S., Huang, M., Shao, X., Mickler, R. A., Li, K., and Ji, J. (2004). Vertical distribution of soil organic carbon in China. *Environ. Manag.* 33, 200–209. doi:10.1007/s00267-003-9130-5

Wei, H., Zhang, K., Zhang, J., Li, D., Zhang, Y., and Xiang, H. (2018). Grass cultivation alters soil organic carbon fractions in a subtropical orchard of southern China. *Soil Tillage Res.* 181, 110–116. doi:10.1016/j.still.2018.04.009

Weissert, L. F., Salmond, J. A., and Schwendenmann, L. (2016). Variability of soil organic carbon stocks and soil CO2 efflux across urban land use and soil cover types. *Geoderma* 271, 80–90. doi:10.1016/j.geoderma.2016.02.014

Wu, X., Zang, S., Ma, D., Ren, J., Chen, Q., and Dong, X. (2019). Emissions of CO2, CH4, and N2O fluxes from forest soil in permafrost region of daxing'an mountains, northeast China. *Int. J. Environ. Res. Public Health* 16, 2999. doi:10.3390/ijerph16162999

Xu, H., Cai, A., Wu, D., Liang, G., Xiao, J., Xu, M., et al. (2021). Effects of biochar application on crop productivity, soil carbon sequestration, and global warming potential controlled by biochar C:N ratio and soil pH: a global meta-analysis. *Soil Tillage Res.* 213, 105125. doi:10.1016/j.still.2021.105125

Xu, L., Deng, X., Ying, J., Zhou, G., and Shi, Y. (2020). Silicate fertilizer application reduces soil greenhouse gas emissions in a Moso bamboo forest. *Sci. Total Environ.* 747, 141380. doi:10.1016/j.scitotenv.2020.141380

Yang, M., Li, Y., Li, Y., Chang, S. X., Yue, T., Fu, W., et al. (2017). Effects of inorganic and organic fertilizers on soil CO2 efflux and labile organic carbon pools in an intensively managed moso bamboo (phyllostachys pubescens) plantation in subtropical China. *Commun. Soil Sci. Plant Analysis* 48, 332–344. doi:10.1080/00103624.2016.1269802

Yang, S., Yang, D., Shi, W., Deng, C., Chen, C., and Feng, S. (2023). Global evaluation of carbon neutrality and peak carbon dioxide emissions: current challenges and future outlook. *Environ. Sci. Pollut. Res.* 30, 81725–81744. doi:10.1007/s11356-022-19764-0

Yuan, N., Wang, E., Lv, S., Tang, X., Wang, T., Wang, G., et al. (2023). Degradation reduces greenhouse gas emissions while weakening ecosystem carbon sequestration of Moso bamboo forests. *Sci. Total Environ.* 877, 162915. doi:10.1016/j.scitotenv.2023.162915

Zhang, F., and Qian, H. (2024). A comprehensive review of the environmental benefits of urban green spaces. *Environ. Res.* 252, 118837. doi:10.1016/j.envres.2024.118837

Zhang, J., Li, Y., Chang, S. X., Qin, H., Fu, S., and Jiang, P. (2015). Understory management and fertilization affected soil greenhouse gas emissions and labile organic carbon pools in a Chinese chestnut plantation. *For. Ecol. Manag.* 337, 126–134. doi:10.1016/j.foreco.2014.11.004

Zhang, J., Tian, H., You, Y., Liang, X. Z., Ouyang, Z., Pan, N., et al. (2024a). Balancing non-CO2 GHG emissions and soil carbon change in U.S. Rice paddies: a retrospective meta-analysis and agricultural modeling study. *AGU Adv.* 5, 1–28. doi:10.1029/2023AV001052

Zhang, X., Huang, H., Tu, K., Li, R., Zhang, X., Wang, P., et al. (2024b). Effects of plant community structural characteristics on carbon sequestration in urban green spaces. *Sci. Rep.* 14(1), 7382. doi:10.1038/s41598-024-57789-2

Zhang, Z., Wang, T., Skidmore, A. K., Cao, F., She, G., and Cao, L. (2023). An improved area-based approach for estimating plot-level tree DBH from airborne LiDAR data. *For. Ecosyst.* 10, 100089. doi:10.1016/j.fecs.2023.100089

Zhu, J., Wang, C., Zhou, Z., Zhou, G., Hu, X., Jiang, L., et al. (2020). Increasing soil carbon stocks in eight permanent forest plots in China. *Biogeosciences* 17, 715–726. doi:10.5194/bg-17-715-2020